

Exchange interactions and critical temperatures in diluted magnetic semiconductors

J Kudrnovský^{1,2}, V Drchal¹, I Turek^{3,4}, L Bergqvist⁵, O Eriksson⁵,
G Bouzerar⁶, L Sandratskii² and P Bruno²

¹ Institute of Physics, Academy of Sciences of the Czech Republic, Na Slovance 2, CZ-18221 Prague 8, Czech Republic

² Max-Planck Institut für Mikrostrukturphysik, Weinberg 2, D-06120 Halle, Germany

³ Institute of Physics of Materials, Academy of Sciences of the Czech Republic, Žitkova 22, CZ-61662 Brno, Czech Republic

⁴ Department of Electronic Structures, Charles University in Prague, Ke Karlovu 5, CZ-12116 Prague 2, Czech Republic

⁵ Department of Physics, University of Uppsala, Box 530, SE-75121, Uppsala, Sweden

⁶ Institute Laue-Langevin, BP 156, F-38042, Grenoble, France

E-mail: kudrnov@fzu.cz

Received 15 April 2004

Published 19 November 2004

Online at stacks.iop.org/JPhysCM/16/S5571

doi:10.1088/0953-8984/16/48/013

Abstract

A first-principles approach to magnetic properties of diluted magnetic semiconductors (DMS) is presented that is based on the local spin-density approximation (LSDA) as implemented in the framework of the tight-binding linear muffin-tin orbital method, while the effect of randomness is described by the coherent potential approximation. Application of a real-space Green-function formalism yields the exchange pair interactions between distant magnetic atoms that are needed for quantitative studies of magnetic excitations including the Curie temperatures. We have found that the pair exchange interactions exhibit a strong directional dependence and are exponentially damped with increasing distance between magnetic atoms due to disorder and the half-metallic character of the DMS. As a case study we consider (Ga, Mn)As, (Ga, Mn)N, and (Zn, Cr)Te alloys. The calculations demonstrate that inclusion of disorder and, in particular, realistic distances among magnetic impurities, are needed to obtain critical temperatures which are in good agreement with available experiments.

1. Introduction

The diluted III–V magnetic semiconductors (DMS) are materials which exhibit spontaneous ferromagnetism mediated by holes in the valence band of the host semiconductor and thus represent new materials with promising applications in spintronics. They have attracted a

great deal of attention from both the experimental and theoretical points of view (for a recent review see [1]). In this paper we present a first-principles study of pair exchange interactions as a function of both the distance between magnetic atoms and the impurity concentrations. The knowledge of these exchange interactions allows one to address in detail the character of magnetic excitations in the DMS, i.e. to evaluate the Curie temperature, the spin-wave stiffness and the spectrum of low-lying magnetic excitations. Magnetic excitations in ferromagnets are of two different kinds, namely, Stoner excitations associated with longitudinal fluctuations of the magnetization, and spin-waves, or magnons corresponding to collective transverse fluctuations of the magnetization direction. The low-temperature regime is dominated by magnons and Stoner excitations can be neglected.

We adopt a two-step procedure [2] which consists in mapping of the complicated itinerant electron system onto an effective random Heisenberg Hamiltonian with classical spins and a consequent application of statistical mechanical methods. The validity of this approach, based on the adiabatic approximation, is in particular justified for magnetic atoms with large exchange splittings, like, e.g., Mn- and Cr-impurities. The mapping is further simplified by using the magnetic force-theorem [2, 3] for an estimate of corresponding total-energy differences between the excited and ground states. We have calculated first-principles effective pair exchange interactions in real space for bulk transition metals [4] and rare-earth metals [5, 6] as well as for low-dimensional systems such as ultrathin films [7] and used these interactions to estimate Curie temperatures and magnon spectra which were in a good agreement with available experimental data. Recently we have also extended this approach to random systems, in particular to the DMS, where the effect of disorder due to impurities is treated in the framework of the coherent potential approximation (CPA) [8, 9]. Alternatively, the two-step approach can be implemented in the framework of the reciprocal-space, frozen-magnon approach, where the effect of impurities is included using the supercell approach [10].

2. Formalism and numerical details

We have determined the electronic structure of the DMS in the framework of the first principles all-electron tight-binding linear muffin-tin orbital method (TB-LMTO) method in the atomic-sphere approximation (ASA) using empty spheres in the interstitial tetrahedral positions of the zinc-blende lattice needed for a good space filling. We used equal Wigner–Seitz radii for all sites. The valence basis consists of s-, p- and d-orbitals; we included scalar-relativistic corrections but neglected spin–orbit effects. Substitutional disorder due to various impurities, both magnetic and non-magnetic, is included by means of the CPA. Charge selfconsistency is treated within the framework of the local spin density approximation (LSDA) using the Vosko–Wilk–Nusair parametrization for the exchange–correlation potential. The experimental lattice constants of the host semiconductor are also used for the DMS alloys but we have verified that we can neglect a weak dependence of the sample volume on defect concentrations. Further details of the method can be found in [11]. In the supercell approach we replace one cation atom per supercell by a magnetic impurity while the size of the supercell determines the impurity concentration. We employ again the ASA and the concept of empty spheres. Further details can be found in [10].

The exchange interactions were investigated in the framework of an effective (random) Heisenberg Hamiltonian with classical spins

$$H_{\text{eff}} = - \sum_{\mathbf{R}\mathbf{R}'} J_{\mathbf{R}\mathbf{R}'} \mathbf{e}_{\mathbf{R}} \cdot \mathbf{e}_{\mathbf{R}'}, \quad (1)$$

where the subscript \mathbf{R} labels the lattice sites, the vectors $\mathbf{e}_{\mathbf{R}}$ are unit vectors pointing in the direction of the individual local moments, and $J_{\mathbf{R}\mathbf{R}'}$ are the random effective exchange

interactions between a pair of magnetic atoms M and M' situated at sites \mathbf{R} and \mathbf{R}' . The configurationally averaged exchange interactions can be calculated using the magnetic force theorem [2, 3] applied within the TB-LMTO-CPA method [9] and the result is

$$\bar{J}_{\mathbf{R}\mathbf{R}'}^{M,M'} = -\frac{1}{8\pi i} \int_C \text{tr}_L \left[\Delta_{\mathbf{R}}^M(z) \bar{g}_{\mathbf{R}\mathbf{R}'}^{MM',\uparrow}(z) \Delta_{\mathbf{R}'}^{M'}(z) \bar{g}_{\mathbf{R}\mathbf{R}'}^{M'M,\downarrow}(z) \right] dz. \quad (2)$$

In (2), the symbol tr_L denotes the trace over the angular momentum index $L = (\ell m)$ and energy integration is performed in the complex energy plane along a closed contour C starting and ending at the Fermi energy (with the occupied part of the valence band lying inside C). The quantities $\bar{g}_{\mathbf{R}\mathbf{R}'}^{MM',\sigma}(z)$ (σ being a spin index, $\sigma = \uparrow, \downarrow$) denote the site-off-diagonal blocks of the conditionally averaged auxiliary Green-function matrices with elements $\bar{g}_{\mathbf{R}L,\mathbf{R}'L'}^{MM',\sigma}(z)$, i.e. the configurationally averaged quantities with magnetic atoms M and M' fixed at sites \mathbf{R} and \mathbf{R}' , respectively. Finally, $\Delta_{\mathbf{R}}^M(z) = P_{\mathbf{R}}^{M,\uparrow}(z) - P_{\mathbf{R}}^{M,\downarrow}(z)$ are diagonal matrices defined via the potential functions $P_{\mathbf{R}\ell}^{M,\sigma}(z)$ of the TB-LMTO-ASA method for magnetic atoms and closely related to the exchange splittings. The ferromagnetic (antiferromagnetic) couplings correspond to positive (negative) values of $J_{\mathbf{R}\mathbf{R}'}^{M,M'}$. It should be noted that the local environment effects in the Green function matrices $\bar{g}_{\mathbf{R}L,\mathbf{R}'L'}^{MM',\sigma}(z)$, which enter (2), can be safely neglected in the metallic regime of the DMS considered here, i.e. if the Fermi energy lies inside the valence band. The numerical evaluation of the integral (2) requires careful energy and Brillouin zone integrations, in particular when the asymptotic properties (distant \mathbf{R} and \mathbf{R}') are studied.

It can be shown [9] that exchange interactions $J_{\mathbf{R}\mathbf{R}'}^{M,M'}$ in DMS are exponentially damped due to:

- (i) the disorder in random positions of magnetic atoms and the possible presence of other defects as predicted by de Gennes [12], and
- (ii) their half-metallic behaviour, i.e. the situation when the Fermi energy lies inside the majority valence band, but inside the gap of minority states.

It should be noted that damping due to disorder refers to configurationally averaged exchange interactions whereby exchange interactions in each alloy configuration can exhibit a slower decay with distance [13]. The averaged exchange interactions are sampled directly or indirectly in experiments when measuring, e.g., Curie temperatures and spin-wave spectra.

To evaluate the Heisenberg exchange parameters in the framework of the supercell approach we employ the frozen-magnon approach. We calculate the energy of the frozen magnon states $E(\mathbf{q})$ for a regular mesh of the wavevectors \mathbf{q} and use them to determine the Fourier transforms of the interatomic exchange parameters. Performing back Fourier transformation we obtain the J_{ij} parameters.

3. Results

3.1. Exchange interactions

We will discuss first some general properties of $J_{\mathbf{R}\mathbf{R}'}^{Mn,Mn}$. Exchange interactions are anisotropic for different directions as illustrated in figure 1, where we show the dependence of the $\bar{J}_{ij}^{Mn,Mn}$ (multiplied by the RKKY prefactor d^3) with respect to the distance d along the directions [100], [110] and [111] in $(\text{Ga}_{0.95}\text{Mn}_{0.05})\text{As}$ alloy. The dominating character of the exchange interactions along the [110] direction can clearly be seen as well as the smallness of the interactions along the [100] direction. Exchange interactions along the [110] direction dominate even more for $(\text{Ga}_{0.95}\text{Mn}_{0.05})\text{N}$, as shown in the inset. The concentration dependence of exchange interactions in $(\text{Ga}_{0.95}\text{Mn}_{0.05})\text{As}$ along the dominating [110] direction is shown

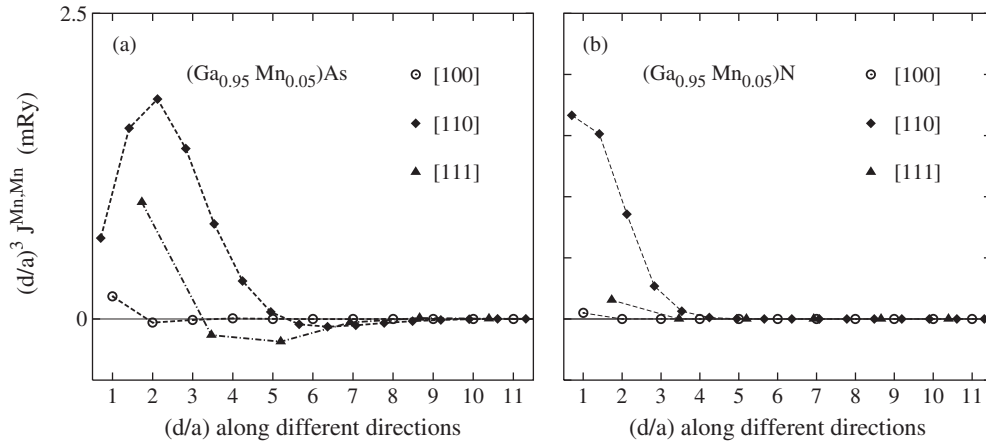


Figure 1. Exchange interactions multiplied by the RKKY prefactor $(d)^3$ and calculated as a function of the distance d (in units of lattice constant a) between two Mn atoms along the [100], [110] and [111] directions: (a) the ferromagnetic $(\text{Ga}_{0.95}\text{Mn}_{0.05})\text{As}$ alloy and (b) the ferromagnetic $(\text{Ga}_{0.95}\text{Mn}_{0.05})\text{N}$ alloy.

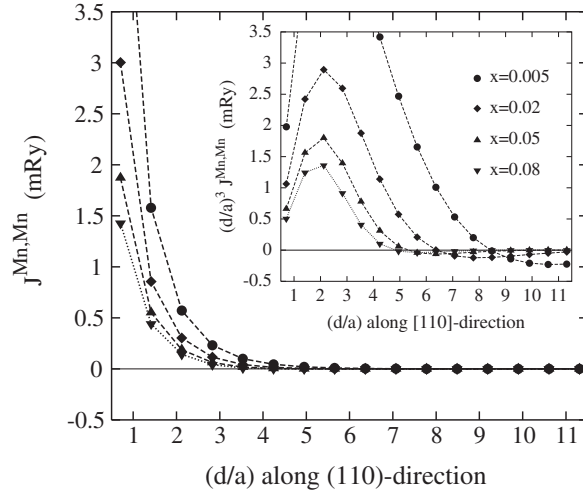


Figure 2. Exchange interactions in ferromagnetic $(\text{Ga}_{1-x}\text{Mn}_x)\text{As}$ calculated as a function of the distance d (in units of lattice constant a) between two Mn atoms along the nearest-neighbour direction [110] for a set of Mn concentrations: $J^{\text{Mn,Mn}}$ (the main frame) and $(d/a)^3 J^{\text{Mn,Mn}}$ (the inset).

in figure 2: exchange interactions are ferromagnetic over larger distances as compared to average distance between two Mn-atoms (about $2.1a$, a is the lattice constant). The exchange interactions are exponentially damped (as clearly illustrated in the inset of figure 3) and their amplitudes are reduced with increasing Mn-concentration. The period of damped oscillations depends inversely proportionally on the size of the Fermi surface, i.e. it increases with decreasing number of carriers (or Mn content). The same effect is seen for increasing doping by As-antisites in $(\text{Ga}_{0.95}\text{Mn}_{0.05})\text{As}$, figure 3, which also reduces the carrier concentration. The strong reduction of the value of the first NN exchange interaction, which for even larger As-concentration changes its sign, indicates the ferromagnetic instability for $y \approx 0.015$ [9].

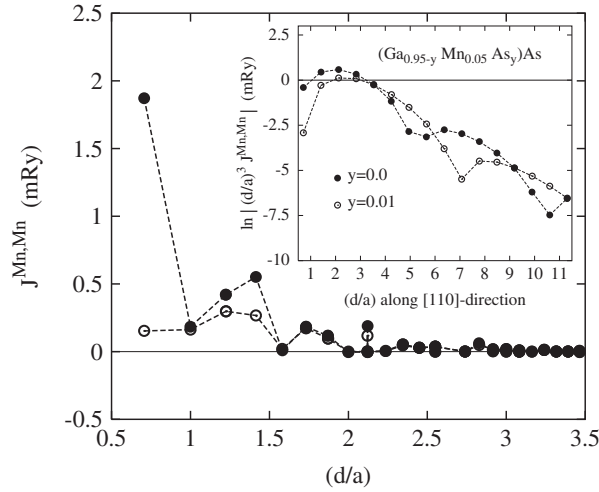


Figure 3. Exchange interactions in ferromagnetic $(\text{Ga}_{0.95-y}\text{Mn}_{0.05}\text{As}_y)\text{As}$ for two different concentrations y of As-antisites plotted as a function of the distance d between two Mn atoms (in units of lattice constant a). Inset: the same but for $\ln |(d/a)^3 \bar{J}^{\text{Mn,Mn}}|$ along the dominating [110] direction.

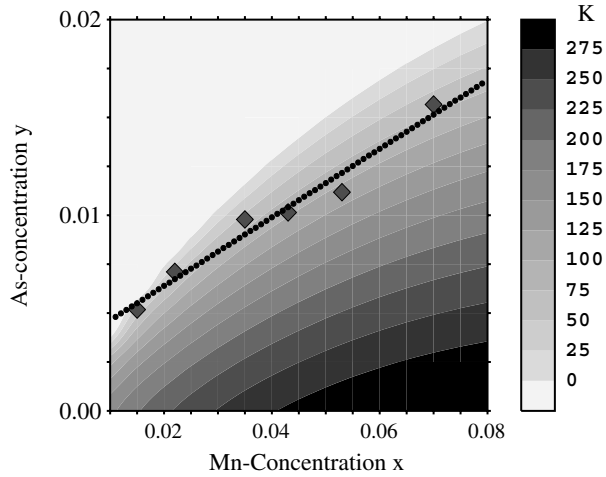


Figure 4. Contour plot of the Curie temperature of ferromagnetic $(\text{Ga}_{1-x-y}\text{Mn}_x\text{As}_y)\text{As}$ as a function of the composition (x, y) . The diamonds refer to experimental values [14], the dotted line represents a least-squares fit to these data.

3.2. Curie temperatures T_c

The simplest mean-field approximation (MFA) for the Curie temperature T_c is directly related to exchange interactions [8, 9], namely, $T_c^{\text{MFA}} = (2x/3) \sum_{\mathbf{R} \neq 0} \bar{J}_{0\mathbf{R}}$, where x is the concentration of magnetic atoms. The lattice is thus an ordered, original one but exchange interactions are simply scaled by concentration x , i.e. the virtual crystal approximation (VCA) is adopted. On the contrary, in the supercell approach we have $T_c^{\text{MFA}} = (2/3) \sum_{\tilde{\mathbf{R}} \neq 0} J_{0\tilde{\mathbf{R}}}$, where the sum runs only over the subset of supercell sites $\tilde{\mathbf{R}}$. The corresponding network of magnetic sites is

Table 1. Critical temperatures of Mn doped GaAs without and with As antisites, Mn doped GaN and Cr-doped ZnTe in kelvins evaluated in the framework of the real-space approach. MFA denotes the mean field result, RPA holds for RPA-VCA, MC-O denotes MC simulations on an ordered network of magnetic atoms (MC-VCA), and MC-R is the main result from MC simulations on a disordered network of magnetic atoms. Expt denotes experimental values.

	(Ga _{0.95-y} As _y Mn _{0.05})As			(Ga _{1-x} Mn _x)N		(Zn _{1-z} Cr _z)Te
	y = 0.0	y = 0.005	y = 0.01	x = 0.03	x = 0.05	z = 0.2
Expt	45–170	45–170	45–170	0–370	0–370	300 ± 10
MFA	287	228	139	342	376	557
MC-O	272	215	131	305	330	491
RPA	275	212	122	293	327	477
MC-R	137	124	92	35	55	301

non-random. On the other hand, the distances are enlarged as compared to the original host cation sublattice.

T_c^{MFA} in Mn-doped GaAs without and with As-antisites (the real-space approach) are shown in figure 4. In qualitative agreement with predictions of model theories [1], T_c increases with the Mn concentration but the presence of antisites strongly reduces it. The same trend and similar values of T_c were also obtained using the frozen-magnon approach [10]. The concentration of As-antisites y in Mn-doped GaAs is not well known from the experiment. A detailed knowledge of T_c as a function of x and y as shown in figure 4, allows us to estimate the relation between x and y in such systems. In figure 4 we have inserted the experimental points for each measured T_c [14] that corresponds to a given x and determined the concentration y such that the calculated and experimental T_c coincide. The data obtained in this way follow approximately a straight line, which in turn suggests that the number of As-antisites increases with the concentration of Mn-atoms in experimental samples. A recent evaluation of formation energies of the As-antisite defects in (Ga, Mn)As [15] confirms this conclusion.

The role of randomness in the distribution of magnetic atoms, neglected in previous studies (e.g. the MFA [9], the RPA-VCA or Monte Carlo (MC) simulations performed in the framework of the VCA (MC-VCA), i.e. also for a non-random lattice [8]), needs clarification. The low concentration of Mn-impurities, combined with the short-ranged and anisotropic character of the exchange interactions demonstrated above, suggests that the phenomenon of magnetic percolation can be relevant for the evaluation of T_c in the DMS. In table 1 we present Curie temperatures obtained from MC simulations performed on random network of sites, where the effect of magnetic percolations is included. We employed the Metropolis algorithm, the finite size scaling method (8000–27 000 of Mn-atoms), and the critical temperatures were determined using the cumulant crossing method [16]. For completeness we present also results for approximations neglecting disorder (MFA, RPA-VCA and MC-VCA). In all cases, exchange interactions up to the 16th shell were included. Spin-fluctuations, which are relevant for reliable determination of the Curie temperature, are also properly taken into account in the present MC simulations.

The results demonstrate that the magnetic percolation becomes more important for lower concentrations of magnetic impurities and for systems with exchange interactions strongly localized in real space (Mn-doped GaN versus Mn-doped GaAs, see figure 1). Only the MC simulations that assume a realistic, random distribution of magnetic atoms give ordering temperatures that are either in a good agreement with experiment or that lie within the range of experimentally observed ordering temperatures. Our study also explains the large range of

Table 2. The mean-field critical temperatures of Mn doped GaAs [10] and GaN [17], and Cr-doped ZnTe [18] in kelvins evaluated in the framework of the supercell approach. Concentrations $x = 0.03125$, $x = 0.0625$ and $z = 0.25$ correspond to supercells with 32, 16 and 4 chemical units, respectively.

$(\text{Ga}_{1-x}\text{Mn}_x)\text{As}$		$(\text{Ga}_{1-x}\text{Mn}_x)\text{N}$		$(\text{Zn}_{1-z}\text{Cr}_z)\text{Te}$
$x = 0.03125$	$x = 0.0625$	$x = 0.03125$	$x = 0.0625$	$z = 0.25$
197	245	83	176	346

experimentally reported ordering temperatures, since the distribution of magnetic atoms on the lattice depends critically on the sample preparation, resulting in a broad range of ordering temperatures.

The MFA values of Curie temperatures obtained from the supercell approach for similar compositions as in table 1 are shown in table 2. Comparing results with experiment as well as with ‘benchmark values’ of MC-R from table 1, we see that the supercell approach is superior to approaches assuming an averaged lattice (VCA). The RPA [10] will further improve agreement with the MC-R results. One can thus conclude that realistic distances among magnetic impurities, properly taken into account in the MC-R approach and approximately in the supercell approach, are of key importance for a correct description of critical temperatures of DMS. Approaches using an average lattice (VCA) should be avoided, in particular for systems with strongly localized exchange interactions, like Mn-doped GaN and also Cr-doped ZnTe.

The present formalism represents a general scheme that can be applied to a number of other problems, like, e.g. the effect of clustering of the magnetic atoms, the effect of interstitial Mn atoms, and its results can serve as a benchmark for analytical theories [19] which take into account the randomness in the Heisenberg Hamiltonian.

Acknowledgments

We acknowledge support from the RTN-Network of the EC *Computational Magneto-electronics* (HPRN-CT-2000-00143). LB and OE acknowledge support from the Swedish Natural Science Foundation (VR), the Swedish Foundation for Strategic Research (SSF), Seagate Inc., the Center for Dynamical Processes Uppsala University, the Göran Gustafsson foundation, and the National Supercomputer Centre (NSC) and High Performance Computing Center North (HPC2N). JK, VD, and IT acknowledge support from the project AVOZ1-010-914 of the Academy of Sciences of the Czech Republic, the Grant Agency of the Academy of Sciences of the Czech Republic (A1010203, S2041105), and the Czech Science Foundation (202/04/0583).

References

- [1] König K, Schliemann J, Jungwirth T and MacDonald A H 2003 *Electronic Structure and Magnetism in Complex Materials* ed D J Singh and D A Papaconstantopoulos (Berlin: Springer) (Preprint cond-mat/0111314)
- [2] Liechtenstein A I, Katsnelson M I, Antropov V P and Gubanov V A 1987 *J. Magn. Magn. Mater.* **67** 65
- [3] Oswald A, Zeller R, Braspenning P J and Dederichs P H 1985 *J. Phys. F: Met. Phys.* **15** 193
- [4] Pajda M, Kudrnovský J, Turek I, Drchal V and Bruno P 2001 *Phys. Rev. B* **64** 174402
- [5] Turek I, Kudrnovský J, Bihlmayer G and Blügel S 2003 *J. Phys.: Condens. Matter* **15** 2771
- [6] Turek I, Kudrnovský J, Diviš M, Franek P, Bihlmayer G and Blügel S 2003 *Phys. Rev. B* **68** 224431
- [7] Pajda M, Kudrnovský J, Turek I, Drchal V and Bruno P 2000 *Phys. Rev. Lett.* **85** 5424
- [8] Bouzerar G, Kudrnovský J, Bergqvist L and Bruno P 2003 *Phys. Rev. B* **68** 205311
- [9] Kudrnovský J, Turek I, Drchal V, Mácá F, Weinberger P and Bruno P 2004 *Phys. Rev. B* **69** 115208
- [10] Sandratskii L M and Bruno P 2002 *Phys. Rev. B* **66** 134435

-
- [11] Turek I, Drchal V, Kudrnovský J, Šob M and Weinberger P 1997 *Electronic Structure of Disordered Alloys, Surfaces and Interfaces* (Boston, MA: Kluwer–Academic)
 - [12] de Gennes P J 1962 *J. Phys. Radium* **23** 630
 - [13] Levy P M, Maekawa S and Bruno P 1998 *Phys. Rev. B* **58** 5588
 - [14] Ohno H 1999 *J. Magn. Magn. Mater.* **200** 110
 - [15] Mašek J, Turek I, Drchal V, Kudrnovský J and Mácá F 2002 *Acta Phys. Polon. A* **102** 673
 - [16] Landau D P and Binder K 2000 *A Guide to Monte Carlo Simulations in Statistical Physics* (Cambridge: Cambridge University Press)
 - [17] Sandratskii L M, Bruno P and Kudrnovský J 2004 *Preprint cond-mat/0404163*
 - [18] Sandratskii L M and Bruno P 2004 *J. Phys.: Condens. Matter* **15** L585
 - [19] Bouzerar G and Bruno P 2002 *Phys. Rev. B* **66** 014410